2014 International Joint Conference on Neural Networks (IJCNN)
July 6-11, 2014, Beijing, China

Motor imagery classification for Brain-Computer Interfaces through a chaotic neural network

Denis Renato de Moraes Piazentin and Joao Luis Garcia Rosa, *Member, IEEE*

***Abstract*— In this paper, we propose to enhance the detection of control states in online brain-computer interfaces (BCI) with the use of the biologically inspired K-set neural network. This neural network was initially built to model brain waves of small sets of neurons in the brain and later showed a great capability of encoding complex and noisy data into oscillation patterns. We apply the K-set network to classification of motor imagery, a type of mental state very useful for BCI applications. Experimental results show that the network can work efficiently in this task and thus provide better control for BCI applications.**

I. INTRODUCTION

BRAIN-COMPUTER INTERFACES (BCI) are systems that transform signals from the brain into a control signal used to control an electronic device, such as a wheelchair or a prosthesis. The task of classification of brain signals is difficult, for presenting low signal to noise ratio, non-linearity and typically, limited training data due to difficulties in collecting signals. Different methods for capturing brain signals are used: electroencephalography (EEG), magneto electroencephalography (MEG), and functional magnetic resonance imaging (fMRI). EEG is the method most commonly used to monitor brain activity because it is non-invasive, it does not require surgical intervention, and it is less expensive than the other alternatives.

For the use of BCI, it is important that the signals used for control be significantly related to specific states of the brain which can be created by the user independently. Various brain states related signals have been used for BCI control, such as P300, motor imagery and finger movement. We focus on motor imagery (MI) which is the mental rehearsal of a motor act without actual movement, as it provides important means for BCI to compensate loss motor functions and has been shown that naive subjects can operate BCI systems based on MI.

A typical practical BCI application has one or more control states, i.e. expected MI events related with some command, and various non-control states, states where there are no command associated and thus the system should ignore the input. Separation of control and non-control states is difficult because there are large within-class variations in non-control, where the brain is not as well controlled as during MI and the BCI must account for that in order to avoid false detection of control states.

Denis Renato de Moraes Piazentin and Joao Luis Garcia Rosa are with the BioCom - Bioinspired Computing Laboratory, Department of Computer Science, University of Sao Paulo, Brazil (emails: {denisrmp, joaoluis}@icmc.usp.br).

K-sets are chaotic neural networks based on the olfactory bulb function, created to model the functioning of different scales of collections of neurons. Although not created for classification problem, the networks have been applied to many different hard problems showing that their ability to encode complex patterns in an attractor landscape is useful, specially in situations where there are only few examples of nonlinear data with low signal to noise ratio. Such data are characteristic of the BCI classification problem, where the cost of acquisition of large training datasets is prohibitive and the low power of the signal (μV for the EEG) together with multiple activities of the body cause a low signal to noise ratio.

The rest of this paper is structured as follows. In section 2, we survey the methods for classifying EEG signals for BCI. In section 3, we review the concepts and workings of K-sets. Finally, in section 4 we present our methods and results. We shall finish with conclusions.

II. EEG SIGNALS

A. EEG and Motor Imagery

EEG consists of a non-invasive technique that allows monitoring the cognitive behavior of humans and animals. EEG is typically recorded with an array of electrodes put on the scalp in a pre-defined pattern, which register oscillations of the electric potentials generated by the brain during cognitive processes. This electrical activity is generated by the interaction of thousands or millions of neurons through the activation of their synapses [1].

The result of the cognitive process is that these potentials recorded by EEG generate a series of oscillations. These oscillations are divided and classified in the EEG rhythms according to their frequency and relation with distinct cognitive processes [2].

Some important rhythms are the α rhythm, within the frequency range of 8 to 12 Hz, related to a relaxing state and recorded in the occipital area of the brain; the β rhythm (13-30 Hz), related to an attention state; the δ rhythm (1-4 Hz), related to profound sleep, and the μ rhythm (8-12 Hz), recorded over the sensorimotor area of the brain and related to motor movement and imagery.

The μ rhythm is the most important for the identification and classification of motor movement and imagery because it is recorded next to brain area responsible for movement [3]. Motor imagery consists of processing from long-term memory to short term or working memory of a motor information, in a process similar to that of remembering or imagining a motor movement.

978-1-4799-1484-5/14/$31.00 ©2014 IEEE

Motor movement and motor imagery cause the phenomena of event related desynchronization (ERD) and event related synchronization (ERS) that make the neurons in the related areas desynchronize the activation of their synapses and then return synchronizing, respectively, and that changes the electric potentials recorded by the electrodes in the scalp, which makes the identification of these events and their classification possible [4].

The magnitude and size of the ERD reflect the size of the mass of neurons involved in a task, so more complex tasks cause major ERDs. ERSs are short-term events correlated with inactivity located in the cortex. For example, during a visual task, such as reading, the sensorimotor cortex responsible for the hands is not necessary, and therefore it is expected to see an increase in μ rhythms and frequencies β in this area. There is also variation in the space-time pattern created by ERDs and ERSs for different events, such as between the movement of the left and right hands. This variation is dependent on the individual and may vary at the site of activation or frequency band, for example [5].

ERS and ERD provide information about the start and the end of the motor movement and have different spatiotemporal patterns according to the planned movement, which allows these events to be identified from the EEG [4]. Motor imagery causes desynchronization in the highest part of the μ rhythm and lower β rhythm next to sensorimotor areas, located at the position of electrodes C3, C4 and CZ in EEG. Figure 1 shows the position of those electrodes following the 10-20 system. For hands movement, desynchronization begins about 2 seconds before the beginning of the movement on the contralateral region of the sensorimotor and becomes bilaterally symmetrical immediately before execution of the movement [6]. The feet can cause an ERD in the center area (near electrode CZ), although not so often.

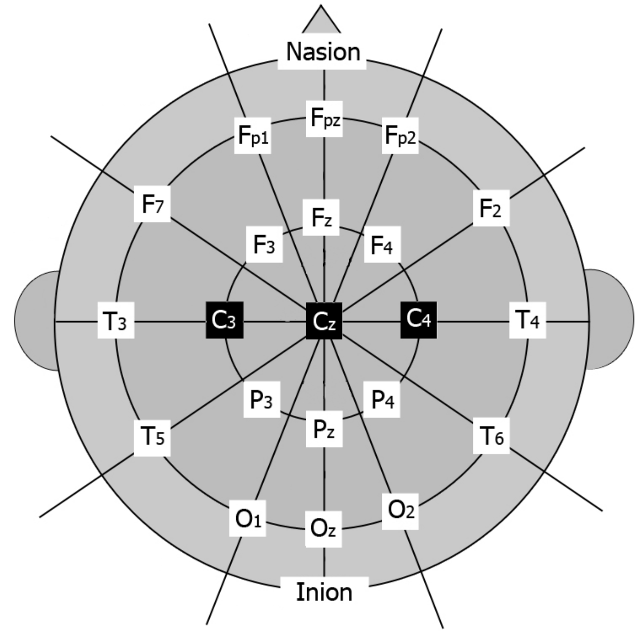

Fig. 1. Positioning of electrodes in scalp following the 10-20 pattern. Electrodes C3, C4 and CZ are located over the sensorimotor area. Based on [7].

B. Classification Algorithms

The classification of EEG signals usually occurs in two steps: the pre-processing of the signal and the classification. The pre-processing can itself be separated in two tasks, removal of artifacts and dimensionality reduction or feature selection.

Artifacts are unwanted electric potentials recorded within the EEG signal that can contaminate and hamper its interpretation [8]. Although there are numerous methods for artifact removal in EEG, as for the motor imagery task the artifacts are in different frequencies than the events of interest. The artifacts are more pronounced below 4Hz and over 30Hz, with μ and β rhythms for motor imagery being from 8 to 20 Hz. Thus, a simple pass band filter suffices for the removal of most artifacts.

The application of dimensionality reduction methods has as objective to reduce the large dimension of data obtained from the EEG signal that can be recorded with sampling of up to 1000 Hz by dozens of electrodes, and by doing this, it keeps only the more relevant features for classification of the signal. The common spatial pattern (CSP) algorithm is currently one of the more successful and accepted methods for dimensionality reduction for motor imagery classification [9].

For the EEG classification, with or without the pre-processing phase, some of the most diverse methods used are the linear discriminant analysis, support vector machines and neural networks as RBF and multi-layer perceptron.

C. Problems

Most of EEG classification is performed in non-continuous, synchronous mode, but applications that are more practical need the processing to occur continuously and that the system be in charge of new inputs during the use. This brings multiple difficulties as the extra noise coming from other uncontrollable brain processes and from the environment and how to differentiate between the multitude of brain states, most of which never seen by the system, with no associated control and reject them, while effectively detecting and classifying control states.

Asynchronous processing of EEG is an actual challenge for the BCI development [9] as improvements in that task can make possible the widespread of BCI systems in real world situations, as the control of prosthesis and wheelchairs for impaired people.

III. K-SET NEURAL NETWORK

A. K-set Hierarchy

Walter Freeman created K-sets in 1975 through the observations he made about the dynamics of populations of neurons in the olfactory system of animals using EEG [10]. The K-sets are biologically more plausible neural networks that have as characteristics the good resistance to noisy data and generalization capabilities even in complex and non-linear environments with few examples.

K-sets are organized in an increasing complexity hierarchy that ranges from K0 to KV, where the more complex levels are built from the simpler ones.

The more basic level is the K0 that represents a population of $10,000$ neurons and it is biologically motived by the structure of columns of neurons in the brain. K0 is the basic building block for the K-sets and is modeled after the mean population impulse response of a population observed in the post-synaptic potential by an ordinary differential equation:

$$\frac{1}{ab}\left[\frac{d^2x_i(t)}{d^2t}+(a+b)\frac{dx_i(t)}{dt}+abx_i(t)\right]=f(t) \qquad (1)$$

where $a = 0.22$ and $b = 0.72$ are temporal constants of biologic populations of neurons and represent the passive membrane time and dispersion delays and x_i is the activation of the i-th population of neurons. The input for a K0 is given by:

$$f(t)=\sum_{j\neq i}^{N}[W_{ij}\times Q(x_j(t),q)]+I_i(t) \qquad (2)$$

where N is the number of populations, W is the vector of weights representing the connection between the populations i and j, t is the time, I is an external stimuli received, for example, from olfactory nerves or, in the model, from the network input. $Q(x(t),q)$ is a sigmoid function that models the transformation between waves and pulses in neuron activations [11] and is given by:

$$Q(x,t)=q(1-e^{-(e^{x(t)}-1)/q}) \qquad (3)$$

where $q = 5$ is the typical value in awake animals and simulations.

K0 dynamics are governed by a zero point attractor and stays in equilibrium except when perturbed.

The KI, one level above K0 in the hierarchy, models the interaction between populations of neurons of the same type and is built by two units of K0 connected through either excitatory or inhibitory connections. The KI shows a form of simple feedback between neuron populations and is able to sustain input for more time. Figure 2 shows the impulse response for K0, KI, and KII model.

The KII is built through at least two KI or four K0 heavily connected and models the interaction between excitatory and inhibitory populations. The interaction between populations of inverse polarities makes the KII form several types of oscillators according with the configuration of its connections [12]. The type of attractor formed varies greatly from the weight parameters.

KIII is biologically motivated by the olfactory system. The KIII is built from three layers of interconnected KII. The first layer corresponds to the olfactory bulb (OB) and has a size of N, where N is the dimension of the input of the network. The OB then connects to the second and third layers, the anterior olfactory nuclei (AON) and the pre-piriform cortex (PC). AON and PC then have connections

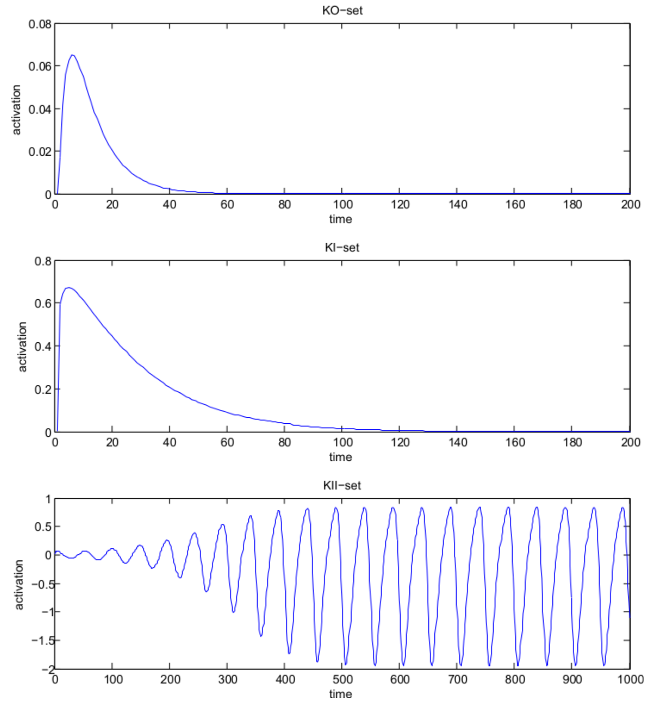

Fig. 2. Impulse response for K0, KI, and KII model. KI is able to sustain impulse for a longer period of time, while KII converges to an oscillator.

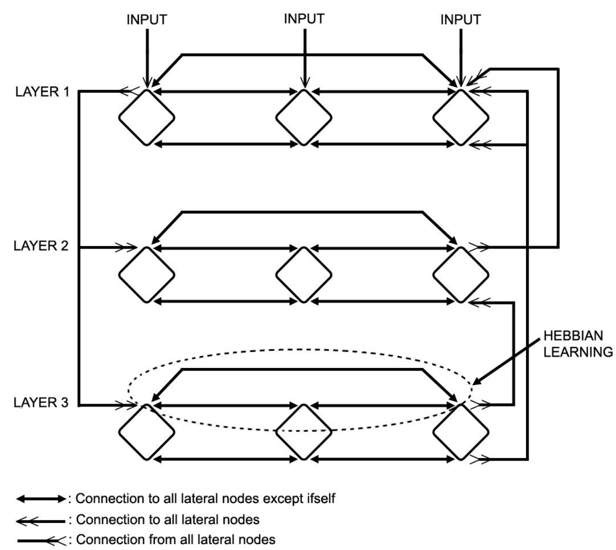

Fig. 3. Generic structure of a KIII neural network with size 3. Input comes into the top layer and is projected onto deeper layers. Feedforward projections are immediate and feed-back projections are time delayed. Intra-layer lateral connections are immediate. Hebbian learning occurs in the lateral connections of the third layer. Based on [14].

between themselves and back to the OB [13] (see Figure 3). As the output is dispersed in the PC layer of the KIII, a second algorithm is typically used to translate or classify this output. The algorithms most commonly chosen for this task are the k-nearest neighbors and the linear discriminant analysis.

Learning in KIII is done through the Hebbian learning rule. The Hebbian rule is used to adapt the weights of the excitatory connections between KII-sets and is modified for use in K-sets, due to the activations being represented as continuous oscillations. The standard deviation σ from each oscillating unit is computed over a time T, where T is usually half of the active phase. The mean standard deviation $\bar{\sigma}$ of the vector $\vec{\sigma}$ of deviations is then computed.

The weight update in the connection between two K0 units $K0_p$ and $K0_q$ is then given by

$$w_{pq} = w_{pq} + \Delta w_{pq} \tag{4}$$

where

$$\Delta w_{pq} = \begin{cases} \alpha(\sigma_p - \bar{\sigma})(\sigma_q - \bar{\sigma}), & \text{if } \sigma_p > \bar{\sigma}, \sigma_q > \bar{\sigma} \\ 0, & \text{otherwise} \end{cases} \tag{5}$$

where α is a learning rate constant.

B. Chaotic Model

Freeman's observations on the brain suggest that chaos plays a fundamental role in cognition. Chaotic systems can create exciting patterns of activity, they can jump from one mode of behavior to another instantly, which reflects the fact that it has a collection of attractors and can easily switch between them. Brains are wired in a manner that chaotic attractors function as representation of internal memories, concepts and actions and the continuous processing of brain occurs through a constant switching between a receiving mode to a transmitting mode [15].

The Freeman K-sets models simulate the chaotic dynamics of the olfactory system [10]. In the absence of stimuli, the system stays in a high dimensional state of basal activity, governed by an aperiodic and non-convergent global attractor, constrained by a landscape of multiple attractors. When stimuli are presented to the system, it exits the basal state and converges to a local basin of attraction, which is a memory wing and usually has a much lower dimension than the basal state and resides in the this wing for the duration of the stimulus, when it returns to the basal state [16]. K-sets thus encode and store information in patterns of the spatial configuration of the average intensity of neuron activations over a time window that is represented by the sequence of patterns during the burst of stimuli.

The system's memory is defined through the collection of metastable basins and attractor wings and a recall is the induction by a state transition of spatio-temporal oscillation with a sequence of patterns. The learning process is made of two main processes: a fast Hebbian reinforcement learning, in which stimulus patterns are presented to the network and connections from populations that are activated together are reinforced by adapting the connection weights. The second is a process of habituation, that is a slow and cumulative process of weight decay to avoid the saturation of network weights and reduce the influence of irrelevant, confusing, ambiguous or otherwise unwanted stimuli [16].

This memory is robust and allows for fast encoding of complex patterns in the K-sets. K-sets have been shown to be able to learn complex patterns, as non-linear problems, with very few training examples and very fast.

IV. K-SET EEG PROCESSING

The method is evaluated using the BCI Competition IV Dataset I [17] which contains recorded data from 4 human subjects and 3 computer generated artificial data sets. The EEG data contain recordings from fifty-nine channels digitized to 1000 Hz and distributed mostly over and around the sensorimotor areas of the brain.

In the dataset, each subject was asked to select between two of three motor imagery tasks: left hand, right hand, and feet. The recording was separated in a session for recording training data and a session for testing data.

Our task is to detect and classify motor imagery in the continuous and multivariate time series of EEG. The expected output is a real number for each time t in the time series, where -1 and 1 are different motor imagery tasks and the resting phase, when there is no intended motor imagery, that should be 0.

First step is feature selection using the filter-bank common spatial pattern technique. Next we train the K-set network and perform the classification.

A. Feature Selection

The primary phenomena observable during motor imagery is the event-related desynchronization (ERD), caused by the blocking in μ and β frequency ranges during the imagery event, and the event-related synchronization (ERS), caused by the posterior unblocking of frequencies. The ERD/ERS phenomena have different spatial characteristics for each observable event. Left hand imagery causes ERD in the right contra-lateral area of the sensorimotor cortex while right hand imagery happens in the left area [18]. Knowing that these events occur in the μ and β ranges we can band pass using a bank of filters and then enhance the signal-to-noise ratio of the events of interest by using the common spatial patterns (CSP) algorithm, as done by [19], [20].

For filtering, we use seven band-pass zero-phase Chebychev Type II filters with central frequencies spaced between 8 to 26, with a Q factor of 1.33 and order 4. We then apply CSP in each one of these filters outputs.

CSP is a data-driven technique to analyze multi-channel data recorded from two classes. CSP then does a decomposition of the signal parametrized by a matrix of weights $W \in \mathbb{R}^C$ that projects the signal epoch $x(t) \in \mathbb{R}^C$ in the surrogate space $x_{CSP}(t) \in \mathbb{R}^C$ as follows:

$$x_{CSP}(t) = W^T x(t). \tag{6}$$

Each column of W is a spatial filter, where the k first and last columns are respectively the ones that maximize more the variance from class 1 and class 2. We use $k = 2$, that gives two spatial filters pairs and an output signal of four channels.

The goal of the spatial filtering is to maximize the variance of the spatially filtered signal under one condition while minimizing it for the other condition. This is achieved by solving the generalized eigenvalue problem

$$R_1 w = \lambda R_2 w \tag{7}$$

where R_1 and R_2 are the covariance matrices of all epochs of x for each class, respectively. See [21] for a thorough review on the subject.

We use the short-term power of the filtered signal as input for the next step in the process [19]

$$z(t) = \int_{t-l}^{t} x_{CSP}^2(\tau) d\tau. \tag{8}$$

were l defines the length of the short-time window. After some experiments, we choose to use $l = 2.5$ seconds.

We then select a subset from the CSP spatial filters W generated for each of the band-pass filters using a criterion based on mutual information. Mutual information feature selection consists of, given an initial set F with d features, finding a subset $S \in F$ with m features that maximize the mutual information $I(S; \Omega)$. For features with continuous input and discrete class, the mutual information between a vector of features $X = X_1, X_2, \ldots, X_d$ and the classes Ω is [20]

$$I(X; \Omega) = H(\Omega) - H(\Omega|X) \tag{9}$$

where

$$H(X) = -\sum_{x \in X} p(x) \log_2 p(x) \tag{10}$$

with $p(.)$ being a probability function and $H(\Omega|X)$ given by

$$H(\Omega|X) = -\int_x \sum_{w=1}^{N_w} p(w|X) \log_2 p(w|X) dx \tag{11}$$

where $w \in \Omega = 1, \ldots, N_w$ and $p(w|X)$ is estimated by the number of samples from the class w over the total of samples. Therefore, for each CSP filtered feature x_i^{CSP} we calculate the mutual information and select the 4 vectors with the larger mutual information.

As the CSP is designed for separating between two classes and the problem has two motor imagery classes and a resting class we do a pair-wise filtering for each pair of classes and aggregate the classes in a joint feature vector.

B. K-set Training and Testing

The features selected are presented to the KIII during the training phase. The network consists of three KII layers of length M, where M is the input length (twelve, one for each feature generated by the preprocessing). The network is trained with the input data until the generation reaches a minimum error in the validation data, thus allowing the formation of robust attractor landscapes that we can use to enhance data classification. The validation data are chosen randomly from the testing signal.

In our experiment, we use a learning rate α of 0.02. In each training generation, samples are presented in a random order during 300 cycles (milliseconds) in the active phase, when the Hebbian reinforcement occurs, followed by an 200 cycles resting phase, without stimuli, that allows for the K-set to return to its basal state and process the next sample.

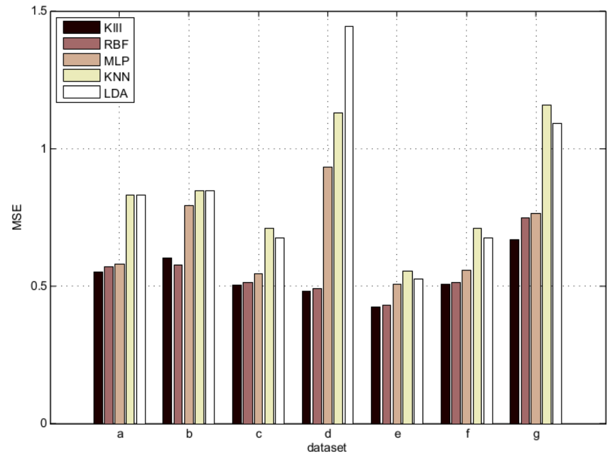

Fig. 4. Mean-squared error for seven datasets with five classification algorithms. Smaller results indicate better classification.

After the training, the samples are again presented to the network, this time without learning, for 300 active cycles and 200 resting cycles. This process consists of recalling the attractor patterns from the network memory. Output from KIII is distributed in the periglomerular layer as KII activations. To provide a single output, we record the activation from each of these samples and use their standard deviation as a feature to train a radial basis function (RBF) algorithm with a single output. We use the standard deviations of all samples as spread parameter in RBF.

V. Experimental Results

Classification step is carried out by mapping the K-sets outputs to the desired output of class labels. We normalize the output to the range [-1 1] and then employ a classification algorithm. We compare the KIII and RBF combination with some widely accepted classification algorithms in EEG classification [22]: multi-layer perceptron (MLP), linear discriminant analysis (LDA), radial-basis function network (RBF), and the k-nearest neighbors algorithm (KNN).

For each one of the seven datasets, experiments were performed. Datasets a, b, f, and g are from real subjects; datasets c, d, and e were artificially generated for the competition. The goal is to clarify how the K-set can improve the performance of motor imagery classification task. For computational efficiency, prediction of class label is performed every 0.5 s.

We evaluate the results using the mean-squared error of class label prediction, the smaller the result is, the best classification is achieved. See table I and figure 4 for a comparison between the results. The classification with KIII is better in 6 out of 7 datasets. Table II shows the average classification error for the four datasets recorded with real subjects. Notice that KIII has the best (smaller) error of the 5 tested algorithms, indicating that it is a good choice for BCI systems based on motor imagery.

TABLE I

MEAN-SQUARED ERROR FOR SEVEN DATASETS WITH FIVE CLASSIFICATION ALGORITHMS. SMALLER RESULTS INDICATE BETTER CLASSIFICATION.

dataset	KIII	RBF	MLP	KNN	LDA
a	**0.5520**	0.5691	0.5790	0.8297	0.8288
b	0.6006	**0.5743**	0.7925	0.8451	0.8456
c	**0.5029**	0.5120	0.5435	0.7105	0.6752
d	**0.4813**	0.4896	0.9325	1.1268	1.4416
e	**0.4206**	0.4286	0.5045	0.5534	0.5243
f	**0.5042**	0.5120	0.5595	0.7105	0.6752
g	**0.6680**	0.7465	0.7629	1.1573	1.0901

TABLE II

AVERAGE CLASSIFICATION ERROR OF THE FOUR REAL DATASETS. SMALLER RESULTS INDICATE BETTER CLASSIFICATION.

	KIII	RBF	MLP	KNN	LDA
average	**0.5812**	0.6005	0.6735	0.8857	0.8599

VI. CONCLUSIONS

In this paper, a biologically motivated neural network, the KIII network, has been applied for motor imagery classification in EEG signals. The experimental results indicate that the KIII can improve the quality of classification, reducing the mean-squared error.

We employed 7 public datasets from the BCI Competition IV for training and testing the KIII model. Comparisons between KIII with other algorithms (RBF, MLP, LDA and KNN) show that the K-model achieves better results in this domain. There is need for future studies to explore improvements of the proposed KIII-based method. Additional motor imagery datasets could also be explored.

ACKNOWLEDGMENTS

Denis Renato de Moraes Piazentin and Joao Luis G. Rosa are grateful to Brazilian Agency FAPESP (processes 2012/15178-7 and 2012/09268-3) for the financial support.

REFERENCES

[1] G. Buzsaki, C. A. Anastassiou, and C. Koch, “The origin of extracellular fields and currents – eeg, ecog, lfp and spikes,” *Nature Reviews Neuroscience*, vol. 13, no. 6, pp. 407–420, june 2012.

[2] P. Nunez and R. Srinivasan, *Electric Fields of the Brain: The Neurophysics of Eeg*. Oxford University Press, 2006.

[3] H. Mizuhara, “Cortical dynamics of human scalp eeg origins in a visually guided motor execution,” *NeuroImage*, vol. 62, no. 3, pp. 1884 – 1895, 2012.

[4] J. R. Wolpaw, N. Birbaumer, D. J. McFarland, G. Pfurtscheller, and T. M. Vaughan, “Brain-computer interfaces for communication and control,” *Clinical Neurophysiology*, vol. 113, no. 6, pp. 767 – 791, 2002.

[5] G. Pfurtscheller, C. Neuper, D. Flotzinger, and M. Pregenzer, “Eeg-based discrimination between imagination of right and left hand movement,” *Electroencephalography and Clinical Neurophysiology*, vol. 103, no. 6, pp. 642 – 651, 1997.

[6] G. Pfurtscheller and F. Lopes da Silva, “Event-related eeg/meg synchronization and desynchronization: basic principles,” *Clinical neurophysiology*, vol. 110, no. 11, pp. 1842–1857, 1999.

[7] S. Sanei and J. Chambers, *EEG Signal Processing*. John Wiley & Sons, 2007.

[8] M. Fatourechi, A. Bashashati, R. K. Ward, and G. E. Birch, “Emg and eog artifacts in brain computer interface systems: A survey,” *Clinical Neurophysiology*, vol. 118, no. 3, pp. 480 – 494, 2007.

[9] M. Tangermann, K.-R. Mller, A. Aertsen, N. Birbaumer, C. Braun, C. Brunner, R. Leeb, C. Mehring, K. J. Miller, G. Mueller-Putz, G. Nolte, G. Pfurtscheller, H. Preissl, G. Schalk, A. Schlgl, C. Vidaurre, S. Waldert, and B. Blankertz, “Review of the bci competition iv,” *Frontiers in Neuroscience*, vol. 6, no. 55, 2012.

[10] W. J. Freeman, *Mass action in the nervous system*, 1st ed. Academic Press, nov. 1975.

[11] R. Ilin and R. Kozma, “Sensor integration in kiv brain model for decision making,” in *Neural Networks, 2009. IJCNN 2009. International Joint Conference on*, june 2009, pp. 1328 –1334.

[12] R. Kozma, J. L. G. Rosa, and D. R. M. Piazentin, “Cognitive clustering algorithm for efficient cybersecurity applications,” in *Neural Networks, 2013. IJCNN 2013. International Joint Conference on*, 2013.

[13] R. Kozma, “Intentional systems: Review of neurodynamics, modeling, and robotics implementation,” *Physics of Life Reviews*, vol. 5, no. 1, pp. 1 – 21, 2008.

[14] R. Ilin and R. Kozma, “Stability of coupled excitatoryinhibitory neural populations and application to control of multi-stable systems,” *Physics Letters A*, vol. 360, no. 1, pp. 66 – 83, 2006.

[15] W. J. Freeman, *How Brains Make Up Their Minds*, 1st ed. Columbia University Press, feb. 2001.

[16] R. Kozma and W. Freeman, “Chaotic resonance-methods and applications for robust classification of noisy and variable patterns,” *International journal of bifurcation and chaos in applied sciences and engineering*, vol. 11, no. 6, pp. 1607–1630, 2001.

[17] B. Blankertz, G. Dornhege, M. Krauledat, K.-R. Muller, and G. Curio, “The non-invasive berlin brain-computer interface: Fast acquisition of effective performance in untrained subjects,” *NeuroImage*, vol. 37, no. 2, pp. 539 – 550, 2007.

[18] G. Pfurtscheller, A. S. Jr., and C. Neuper, “Event-related synchronization (ers) in the alpha band: an electrophysiological correlate of cortical idling: A review,” *International Journal of Psychophysiology*, vol. 24, no. 12, pp. 39 – 46, 1996.

[19] H. Zhang, C. Guan, K. K. Ang, and Z. Y. Chin, “Learning discriminative patterns for self-paced eeg-based motor imagery detection,” *Frontiers in Neuroscience*, vol. 6, no. 7, 2012.

[20] K. K. Ang, Z. Y. Chin, H. Zhang, and C. Guan, “Filter bank common spatial pattern (fbcsp) in brain-computer interface,” in *Neural Networks, 2008. IEEE International Joint Conference on*. IEEE, 2008, pp. 2390–2397.

[21] B. Blankertz, R. Tomioka, S. Lemm, M. Kawanabe, and K.-R. Muller, “Optimizing spatial filters for robust eeg single-trial analysis,” *Signal Processing Magazine, IEEE*, vol. 25, no. 1, pp. 41–56, 2008.

[22] F. Lotte, M. Congedo, A. Lcuyer, F. Lamarche, and B. Arnaldi, “A review of classification algorithms for eeg-based braincomputer interfaces,” *Journal of Neural Engineering*, vol. 4, no. 2, p. R1, 2007.